ISSN 1674-1056
http://cpb.iphy.ac.cn
http://iopscience.iop.org/cpb
中国物理 B
Chinese Physics
中国物理 Chinese Physics B

Numerical tests of theoretical models describing ionization of H(1s) atom by linearly polarized flat pulse of laser radiation

Jarosław H Bauer, Min Deng(邓敏)

Citation: Chin. Phys. B . 2018, 27(9): 093202. **doi:** 10.1088/1674-1056/27/9/093202

Journal homepage: http://cpb.iphy.ac.cn; http://iopscience.iop.org/cpb

What follows is a list of articles you may be interested in

Modulation of multiphoton resonant high-order harmonic spectra driven by two frequency-comb fields

Yuanyuan Zhao(赵媛媛), Di Zhao(赵迪), Chen-Wei Jiang(蒋臣威), Fu-li Li(李福利)

Chin. Phys. B . 2018, 27(5): 053202. **doi:** 10.1088/1674-1056/27/5/053202

Isolated attosecond pulse generation with few-cycle two-color counter-rotating circularly polarized laser pulses

Jin-Song Wu(吴劲松), Zheng-Mao Jia(贾正茂), Zhi-Nan Zeng(曾志男)

Chin. Phys. B . 2017, 26(9): 093201. **doi:** 10.1088/1674-1056/26/9/093201

Semiclassical investigation of Coulomb focusing effects in atomic above-threshold ionization with elliptically polarized laser fields

Chuan-Liang Wang(王传亮), Li-Xin Xia(夏立新), Hong-Bin Yao(姚洪斌), Wen-Liang Li(李文亮)

Chin. Phys. B . 2017, 26(4): 043201. **doi:** 10.1088/1674-1056/26/4/043201

High-order harmonic generation of the N_2 molecule in two-color circularly polarized laser fields

Hui Du(杜慧), Jun Zhang(张军), Shuai Ben(贲帅), Hui-Ying Zhong(钟慧英), Tong-Tong Xu(徐彤彤), Jing Guo(郭静), Xue-Shen Liu(刘学深)

Chin. Phys. B . 2016, 25(4): 043202. **doi:** 10.1088/1674-1056/25/4/043202

Dependence of above-threshold ionization spectrum on polarization directions of two-color laser fields

Liu Min, Guo Ying-Chun, Wang Bing-Bing

Chin. Phys. B . 2015, 24(7): 073201. **doi:** 10.1088/1674-1056/24/7/073201

Numerical tests of theoretical models describing ionization of H(1s) atom by linearly polarized flat pulse of laser radiation*

Jarosław H Bauer[1,†] and Min Deng(邓敏)[2,‡]

[1] *Katedra Fizyki Teoretycznej, Wydział Fizyki i Informatyki Stosowanej Uniwersytetu Łódzkiego, Ul. Pomorska* 149/153, *PL-90-236 Łódź, Poland*
[2] *State Key Laboratory of Low-Dimensional Quantum Physics, Department of Physics, Tsinghua University, Beijing* 100084, *China*

(Received 27 April 2018; revised manuscript received 2 July 2018; published online 28 August 2018)

We derive the well-known Coulomb correction factor for the Gordon–Volkov wave function describing an outgoing electron in the process of ionization in an intense laser field. Although rigorous treatment would limit its use only to laser fields much lower than the so-called barrier-suppression field, it appears that in practice the correction factor may be used also close to and even above this critical value of the laser field. We compare predictions of several analytical expressions describing ionization rate of the hydrogen atom in its ground state in the strong linearly polarized laser field. We also compare ionization probabilities obtained by integrating these ionization rates over a temporal envelope of the laser pulse with predictions based on the exact numerical solution to the time-dependent Schrödinger equation.

Keywords: laser fields, ionization, S-matrix, Coulomb–Volkov wave function

PACS: 32.80.Rm, 33.80.Rv **DOI:** 10.1088/1674-1056/27/9/093202

1. Introduction

The S-matrix theory was used to describe the photodetachment or photoionization in intense laser fields many times.[1–12] Sometimes it is called the Keldysh–Faisal–Reiss (KFR) theory or the strong-field approximation (SFA). With many later modifications and advanced improvements it has been frequently used up to date (for recent reviews see, for example, Refs. [13]–[17]). The S-matrix theory gives very reliable quantitative results for a wide range of intensities and frequencies of the laser field and the problem of multiphoton detachment from a negative ion by a linearly polarized laser field.[12–14] More complicated situation occurs for atoms, because in the final state of the ionized outgoing electron the Coulomb effects, due to remaining positively charged ion, cannot be neglected. About twenty years ago it seemed that there was no analytical theory which is accurate enough in non-perturbative (or even the so-called barrier-suppression) laser fields.[18] However, the authors of Ref. [18] did not mention the Perelomov, Popov, and Terent'ev (PPT) theory,[3–8] which gives reasonable total ionization rates also for atoms. The PPT theory has been improved quite recently[19] by computing the Coulomb correction factor Q. The ionization rate formula obtained in Ref. [19] is a product of Q and ionization rate for electron in the short-range potential (see Eqs. (5)–(7) therein). There exists a simplified version of the PPT theory, namely, the Ammosov, Delone, and Krainov (ADK) theory,[20,21] which gives quantitatively good results only in the so-called tunneling regime (see, for instance, Refs. [22] and [23]). The latter one is characterized by the well-known condition: Keldysh parameter $\gamma < 1$ (see below). The multiphoton ionization prevails if $\gamma > 1$, while tunneling dominates in the opposite case. For optical or infrared laser frequency ω (which is low enough), the ionization may be treated as tunneling through the potential barrier formed by superposition of laser and Coulomb electric fields. If the laser field is stronger, it can reach the so-called barrier-suppression ionization (BSI) regime. The latter one is achieved when the peak laser field F is so strong that the above-mentioned potential barrier is lowered below the level E of the initial state of the atom ($E = -E_{\rm B} < 0$, $E_{\rm B}$ is the binding energy; $\gamma = \omega\sqrt{2E_{\rm B}}/F$). This can be expressed by the following well-known condition:

$$F > F_{\rm BSI} = \frac{E_{\rm B}^2}{4Z} = \frac{Z^3}{16n^4}, \tag{1}$$

where n is the principal quantum number of the initial bound state (n,l,m) (with the usual meaning of the quantum numbers n, l, and m) and Z is the nuclear charge (thus $E_{\rm B} = Z^2/(2n^2)$). (In the present work we use atomic units (a.u.): $\hbar = e = m_{\rm e} = 1$, substituting -1 for the electronic charge. We keep any nuclear charge Z in all the equations given below, but finally, in our numerical calculations, we put $Z = 1$ for the hydrogen atom.) For the H(1s) atom $F_{\rm BSI} = 0.063$ a.u., approximately. Not going into details, other considerations lead to greater critical field strengths, for example, $F_{\rm cr} = 0.15$ a.u.[24,25] or $F'_{\rm cr} = 0.13$ a.u.[26] In this work we are interested only in the H(1s) atom ionized by the strong linearly polarized laser field not greater than about $2.5F_{\rm BSI} = 0.156$ a.u.[27] For the peak laser field it corresponds to the laser intensity $I = F^2 = 8.6 \times 10^{14}$ W/cm^2. It appears that already for intensities above

*Project supported by the University of Łódź.
†Corresponding author. E-mail: bauer@uni.lodz.pl
‡Corresponding author. E-mail: dengm13@mails.tsinghua.edu.cn
© 2018 Chinese Physical Society and IOP Publishing Ltd

$I \approx 4.0 \times 10^{14}$ W/cm^2 the H(1s) atom is fully ionized for 2-10-2 flat laser pulse (see below) of typical optical or infrared frequencies. Since the azimuthal dipole selection rule is $\Delta m = 0$ for linearly polarized radiation, $m = 0$ in this work and the quantum numbers (n,l) are sufficient to describe bound states.

The rest of this paper is organized as follows. In Section 2 we present our analytical calculations. The main result is given in Eq. (7). Although it is very well known and simple,[28–30] we acquire it to fill some gap in the literature in this way. More important are our numerical results that we present in Section 3. Based on exact numerical solutions to the time-dependent Schrödinger equation (TDSE) we compare predictions of five earlier known theories with these *ab initio* results. Our numerical method[31] uses a new generalized pseudospectral technique which is extended to perform an optimal spatial grid discretization, leading to a significant improvement in the quality of the wave function over that obtained by the equal-spacing spatial discretization techniques. Our calculations are based on the length gauge (LG), but they give the same results as the velocity gauge (VG) calculations from QPROP package.[32] In the present work, both theoretically and numerically (TDSE) we describe plane-wave laser field in the nonrelativistic dipole approximation. This means that the magnetic field vector of the laser is zero and the electric field vector of the laser depends only on time. We discuss not only strong-field ionization, but also the role of excited states and excitation of the H(1s) atom. In Section 4 we discuss the comparison between TDSE and analytical results. We also speculate on a few frequently used S-matrix theories from the point of view of their gauge dependence, accuracy and range of applicability. Finally, some conclusions are drawn from the present study in Section 5.

2. Theory

The quasiclassical (WKB) Coulomb correction to the Gordon–Volkov final-state wave function[33,34] was proposed quite a long time ago[28–30] by Krainov *et al.* (but the treatment is analogous to that from the well known PPT theory[3–8]). According to quasi-classical perturbation theory for the Coulomb potential of the atomic nucleus $U(r) = -Z/r$, the Gordon–Volkov final-state wave function should be multiplied by the factor

$$I(r) = \exp\left(-\mathrm{i}\int U\,\mathrm{d}t\right) = \exp\left(-\mathrm{i}\int_r^{r_2} U\left(r'\right)\frac{\mathrm{d}r'}{p\left(r'\right)}\right), \quad (2)$$

where the integral in Eq. (2) is over the path of under barrier electronic motion ($p(r')$ has purely imaginary value), r is the actual electronic position (the same as that in the Gordon–Volkov wave function), and r_2 is this position at the tunnel exit (see below)). The potential barrier is formed on one side of the atom as a result of superposition of two electric fields. The Coulomb potential $U(r)$ and the potential $-Fr$ describe the two fields. The latter one is quasistatic (or slowly varying in time), and F is the peak electric field of the laser plane wave. Assuming further that only moments of the peak laser field dominate during the ionization, one obtains the Coulomb correction, which is constant in time (see the text just above Eq. (2) in Ref. [30]). For the linearly polarized laser field this is another simplification (which has been recently overcome in Ref. [35]). For the circularly polarized laser field there is no such simplification because $|\boldsymbol{F}(t)| = F = \text{const}$ and the result is the same as that for the case of linear polarization. The initial bound state of the atom, described by the quantum numbers (n,l,m), has the total energy $-Z^2/(2n^2)$. Therefore the electron momentum $p(r)$ can be calculated from the following equation (conservation of energy):

$$\frac{p^2(r)}{2} - \frac{Z}{r} - Fr = -\frac{Z^2}{2n^2}. \quad (3)$$

In the above equation one assumes that the field F is weak enough so that the maximum of the potential energy curve $E(r) = -Z/r - Fr$ lies above the level $E = -Z^2/\left(2n^2\right)$. One can easily calculate that this condition is exactly the one given in Eq. (1). The maximum of $E(r)$ occurs for $r_{\max} = \sqrt{Z/F}$. Then the equation $E(r) = -Z^2/\left(2n^2\right) = -E_{\mathrm{B}}$ has two solutions r_1 and r_2, which correspond to points, where the ionized electron enters into and leaves from the potential barrier, respectively

$$r_1 = \frac{1}{2F}\left(E_{\mathrm{B}} - \sqrt{E_{\mathrm{B}}^2 - 4ZF}\right),$$
$$r_2 = \frac{1}{2F}\left(E_{\mathrm{B}} + \sqrt{E_{\mathrm{B}}^2 - 4ZF}\right). \quad (4)$$

The width of the barrier is given as $D = r_2 - r_1 = \sqrt{E_{\mathrm{B}}^2 - 4ZF}/F$. Of course $r_1 < r_{\max} < r_2$, if $F < F_{\mathrm{BSI}}$. If $F = F_{\mathrm{BSI}}$ then $D = 0$ and $r_1 = r_{\max} = r_2 = 4n^2/Z$. To derive our main analytical result here, we assume that

$$F \ll F_{\mathrm{BSI}}. \quad (5)$$

From Eqs. (4) and (5), the asymptotic approximate expressions are obtained to be $D \approx Z^2/\left(2n^2F\right)$, $r_1 \approx 2n^2/Z$, and $r_2 \approx Z^2/\left(2n^2F\right)$. Solving Eq. (3) for $p(r)$, neglecting Coulombic term therein, one obtains $p(r) \approx \mathrm{i}\sqrt{Z^2/n^2 - 2Fr}$. The latter approximation is justified indeed if $r \gg r_1$ and $F \ll F_{\mathrm{BSI}}$. One can calculate the integral from Eq. (2) as follows:

$$I(r) = \exp\left(Z\int_r^{r_2}\frac{\mathrm{d}r'}{r'\sqrt{Z^2/n^2 - 2Fr'}}\right)$$
$$= \exp\left(-n\left[\ln\frac{1+\sqrt{1-2Fr'(n/Z)^2}}{1-\sqrt{1-2Fr'(n/Z)^2}}\right]_r^{r_2}\right). \quad (6)$$

It follows from Eq. (5) that the contribution to the above definite integral from the point r_2 vanishes. Only the contribution from the point r matters ($r \ll r_2$). Expanding the square root in the denominator in Eq. (6) in the Taylor series $(2Fr(n/Z)^2 \ll 1)$, one finally obtains

$$I(r) = \exp\left(-n\left(0 - \ln\frac{2}{Fr(n/Z)^2}\right)\right) = \left(\frac{2Z^2}{n^2Fr}\right)^n. \quad (7)$$

In the present work we use this factor in the WKB Keldysh model (see below). This is the same as the result given (without derivation) in Eq. (2) of Ref. [30] (note that, in general, n is the effective principal quantum number of the initial atomic or ionic state). Strictly speaking, the result from Eq. (7) is only valid for small enough laser field and frequency. Thus, in the S-matrix theory, for the final state of ionized electron instead of the Gordon–Volkov wave function $\Psi^{\mathrm{GV}}(\boldsymbol{r},t)$ (see, for example, Eq. (5) in Ref. [35]) one should use $I(r)\Psi^{\mathrm{GV}}(\boldsymbol{r},t)$ to take into account Coulomb effects. Indeed, such a kind of calculation (for both linear and circular polarization) was used many times by one of us (see, for example, Refs. [35]–[37]). If one is mainly interested in the total ionization rate (neglecting angular and energy distribution), one can make another simplification in Eq. (7). Namely instead of a position of the electron r, one can substitute its average (calculated in the initial bound state). This was utilized in the Becker *et al.*'s paper,[38] where the VG was used. Ionization rate for the H(1s) atom is then equal to the SFA result of Reiss[10] (see Eq. (45) therein) times the factor $1/F^2$.[39] Such a procedure appeared to be quite successful for many different atoms of noble gases and both polarizations of incident laser radiation.[38] However, the logarithmic scale covering many orders of magnitude on the axis of abscissa is usually used to show comparison between theory and experiment (real or numerical) for ionization rates or ion yields.[22,23,38,40] It is therefore worth examining in more detail the agreement between theory and numerical experiment.

On the other hand, if one wants to keep the exact factor in Eq. (7) (with its r-dependence) in the VG, calculations become much more complicated than analogous calculations in the LG.[37] For the H(1s) atom the initial-state wave function effectively becomes that of the zero-range potential (this is true only in the LG). The respective analytical formula describing ionization rate is given in Eq. (32b) of Ref. [36]. In Figs. 3–6 we have called this model the WKB Keldysh model. More accurate treatment of the linear polarization was considered in Ref. [35], where instead of Eq. (7) we use the following factor:

$$I(r,t) = \left(\frac{2Z^2}{n^2F\sin(\omega t+\varphi_0)\,r}\right)^n, \quad (8)$$

with $n = 1$ (and arbitrary initial phase φ_0). We called this model the TDWKB Keldysh model (time-dependent WKB). The respective analytical formula describing ionization rate is given in Eq. (19) of Ref. [35].

3. Numerical results and discussion

In Figs. 1 and 2 we show how the H(1s) atom behaves in a flat pulse as a function of the peak laser intensity for two different laser wavelengths, namely $\lambda = 800$ nm ($\omega = 0.057$ a.u.) and $\lambda = 400$ nm ($\omega = 0.114$ a.u.), respectively. The peak field is constant for 10 cycles with two-cycle $\sin^2$ (of the vector potential $\boldsymbol{A}(t)$) turn-on and turn-off time (so the total duration of nonzero laser field is 14 cycles). Each time we present three curves pertaining to probabilities of the ground state, excitation and ionization of the atom after the end of the pulse. There are results of exact numerical solutions to the TDSE[31] in Figs. 1 and 2. The pulse 2-10-2 was probably seldom used so far in such numerical simulations. We have chosen it because turn-on and turn-off time are much shorter than the flat part of the pulse (of constant intensity, which is assumed to be in S-matrix theories). The H(1s) atom starts to ionize in a significant way below the laser intensity $I \approx 1.0\times10^{14}$ W/cm^2, which corresponds to $F \approx 0.053$ a.u.$< F_{\mathrm{BSI}} \approx 0.063$ a.u. For the lower frequency $\omega = 0.057$ a.u. the excitation is negligible (less than 10%) for all intensities. For the higher frequency $\omega = 0.114$ a.u. (but still $\omega \ll E_{\mathrm{B}} = 0.5$ a.u.), the excitation is much higher and can reach a level of up to 30% near $I = 1.5\times10^{14}$ W/cm^2. Closer analysis of the bound states involved in this process shows (in Fig. 2) that mainly the states with $l = 3$ and $l = 1$ (and some spread in n) are populated. (One should remember that the spectral width is finite even for our quite a long flat pulse.) This denotes three or one net photon absorbtion. Near $I = 3.5\times10^{14}$ W/cm^2 mainly the states with $l = 2$ (and some spread in n) are populated among some 10% of atoms which become excited. Above $I \approx 4.0\times10^{14}$ W/cm^2 ($F \approx 0.107$ a.u.) the H(1s) atom becomes nearly fully ionized. Since we consider only total ionization rates, neither nondipole nor relativistic effects are necessary to properly describe the ionized electron for laser field parameters from Figs. 1 and 2. For example, the highest quiver velocity of the electron ($v = F/\omega$) in the plane-wave laser field is less than 1.9 a.u.$\approx 0.014c$ (c is the speed of light) for $\omega = 0.057$ a.u. and for $\omega = 0.114$ a.u. v is twice smaller. In Ref. [41] the manifestation of nondipole and relativistic effect in strong-field ionization were discussed. For $\omega = 0.057$ a.u. and $F \approx 0.107$ a.u. the Keldysh parameter $\gamma \approx 0.53 > 0.1$. According to Fig. 3(a) from Ref. [41] and the relevant discussion therein, the relativistic and nonrelativistic force (due to laser field) acting on the ionized electron are identical (within the accuracy of the plot). Thus, one could evaluate that the influence of relativistic effect on total ionization rate would be below 1%. A similar opinion, related to a similar range of the

laser field parameters, is expressed in Ref. [23].

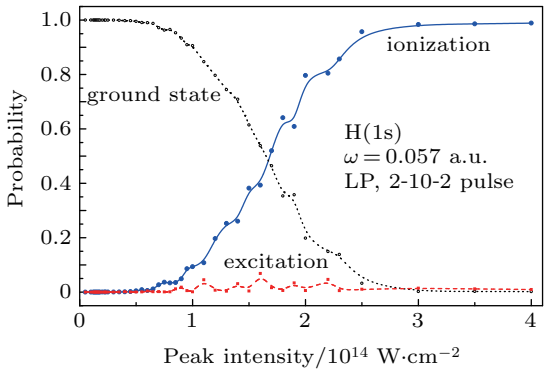


Fig. 1. (color online) Curves of probability of ground state (black dotted curve), ionization (blue solid curve), and excitation (red dashed curve) of the H(1s) atom after the end of the laser pulse versus peak intensity for $\omega = 0.057$ a.u. (Each circle or square corresponds to a single TDSE simulation. B-splines are used to display the curves.)

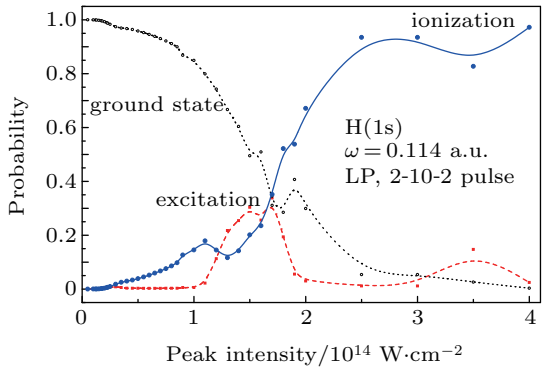


Fig. 2. (color online) The same caption as that of Fig. 1 but for $\omega = 0.114$ a.u.

In Figs. 3 and 4, we show five different theoretical ionization rates as a function of peak electric field of the laser for the same wavelengths, respectively. In our opinion, based on several studies in the literature describing total ionization rates (and some references therein),[18,19,22,23,35–38,40,42] these models describe the rates in the best way. The range of electric fields (displayed in Figs. 3 and 4) corresponds to the range of intensities 3.5×10^{12} W/cm$^2 \leq I \leq 1.4 \times 10^{15}$ W/cm^2. All five curves look qualitatively similar and demonstrate the fast growth of ionization rate with the field increasing. Structures that one sees on the curves relate to the existence of photon thresholds. For instance, at $\omega = 0.114$ a.u. and $F \leq\sim 0.06$ a.u. at least five photons are needed to ionize the atom. With increasing field the channel of five-photon ionization becomes closed and at least six photons are necessary for $F > 0.06$ a.u. Such a channel closing with increasing F usually leads to a local minimum of the ionization rate. There is no pronounced indication after exceeding $F_{\rm BSI}$ (or some other critical field) by F in Figs. 3 and 4. In Fig. 4, the existence of the first local minima on five curves near $F_{\rm BSI}$ relates to the fact that at $F \approx 0.06$ a.u.$\approx F_{\rm BSI}$ the five photon-ionization channel turns closed. Note that the differences among these five theoretical models usually decrease with F increasing and usually increase with ω increasing (cf. also Figs. 1–6 in Ref. [35]).

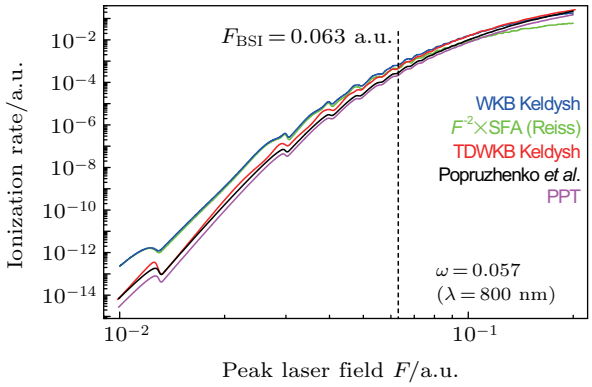


Fig. 3. (color online) Ionization rates for H(1s) atom at laser frequency $\omega = 0.057$ a.u. versus peak laser field F. From top to bottom (for most values of F) curves correspond to five different theories: WKB Keldysh (blue), $F^{-2}\times$ SFA(Reiss) (green), TDWKB Keldysh (red), Popruzhenko *et al.* (black), and PPT (magenta).

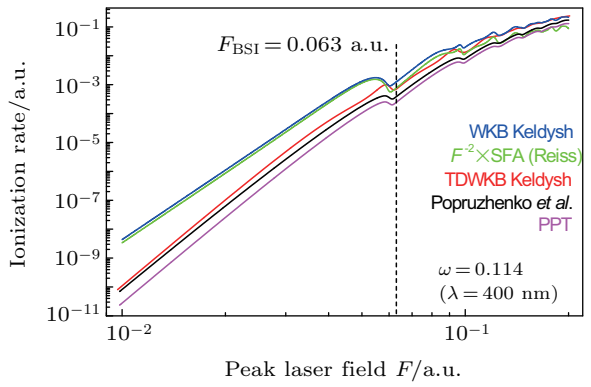


Fig. 4. (color online) The same caption as that of Fig. 3 but for $\omega = 0.114$ a.u.

In Figs. 5(a) and 5(b) we show ionization probabilities after the end of the above mentioned 2-10-2 pulse, as a function of the peak laser intensity for $\omega = 0.057$ a.u. Figures 6(a) and 6(b) are analogous to Figs. 5(a) and 5(b), but $\omega = 0.114$ a.u. We compare the exact numerical solutions to the TDSE (the same as in Figs. 1 and 2) with predictions based on five different theoretical models (the same as in Figs. 3 and 4) describing total ionization rates. The difference between Figs. 5(a) and 5(b) is as follows: in Fig. 5(a) the abscissa and ordinate are both logarithmic, but in Fig. 5(b) the abscissa and ordinate are both linear. Theoretical ionization probabilities are obtained by numerical integration of respective ionization rates over the exact laser pulse profile. This procedure takes into account the depletion effect of the initial state of the atom. In this case the ground state probability and the ionization probability sum up to unity (of course, no excitation can be taken into account here). Logarithmic scales better present numerical data for very small values of ionization probability. One can see that the WKB Keldysh and $F^{-2}\times$ SFA (Reiss) ionization probabilities are in better agreement with the TDSE

results than those from the other three models in Figs. 5(a) and 6(a). For higher peak intensities and ionization probabilities, the agreement between theory and numerical experiment is the best for Popruzhenko *et al.* and PPT theoretical models (cf. Figures 5(b) and 6(b)). Recently introduced TDWKB model usually gives intermediate ionization probabilities and ionization rates (cf. also Figs. 3 and 4).

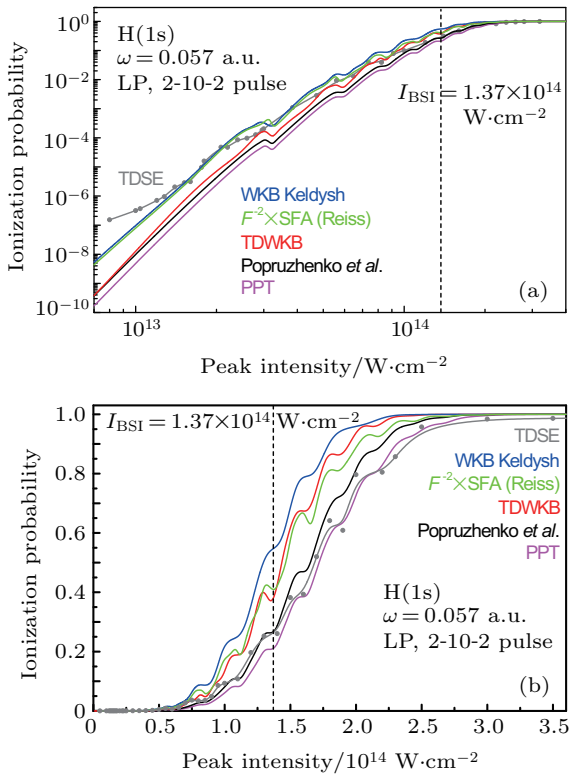


Fig. 5. (color online) Plots of probability of ionization of H(1s) atom after the end of the laser pulse versus peak intensity for $\omega = 0.057$ a.u. Gray solid curve denotes exact numerical TDSE results. Other five curves are obtained by integrating over time ionization rates. Colors of respective curves are the same as in Figs. 3 and 4. There are exactly the same data in Figs. 5(a) and 5(b), where (a) both axes are logarithmical and (b) both axes are linear. TDSE data are the same as those in Fig. 1.

However, for some laser frequencies, the excitation probability may be higher than the ionization probability. In Figs. 7 and 8 we compare these probabilities as a function of frequency for two peak intensities, namely $F = 0.02$ a.u. and $F = F_{\rm BSI} = 0.063$ a.u. under the condition of the same 2-10-2 laser pulse, respectively. In Fig. 7 (for $F = 0.02$ a.u.) both excitation and ionization have comparable values (much smaller than 1) for most laser frequencies. And the ground state probability is almost always very close to unity. The barrier width is $D \approx 20.6$ a.u., hence it is quite large (much larger than the average radius of the atom). In this situation one may neglect the effect of excitation and try to describe the process by simple ionization rate formula. But near $\omega = 0.375$ a.u. the excitation is much stronger than the ionization because this laser frequency is in resonance with one-photon transition between the states $(n,l) = (1,0)$ and $(2,1)$. The energy difference is $E_2 - E_1 = 0.375$ a.u. for these states. One observes a visible hump in excitation probability and a dip in ground state probability. There is another hump for $\omega = E_3 - E_1 = 0.444$ a.u. Again, one-photon transition between the states $(1,0)$ and $(3,1)$ is much more probable than ionization here. In Fig. 8 (for $F = 0.063$ a.u.) the excitation is significant in a frequency range of ~ 0.37 a.u.$\leq \omega \leq \sim 0.47$ a.u., where the states $(2,1)$ and $(3,1)$ are mainly populated. For these frequencies the ionization is much weaker than the excitation. One also observes two other visible humps in the excitation curve for lower

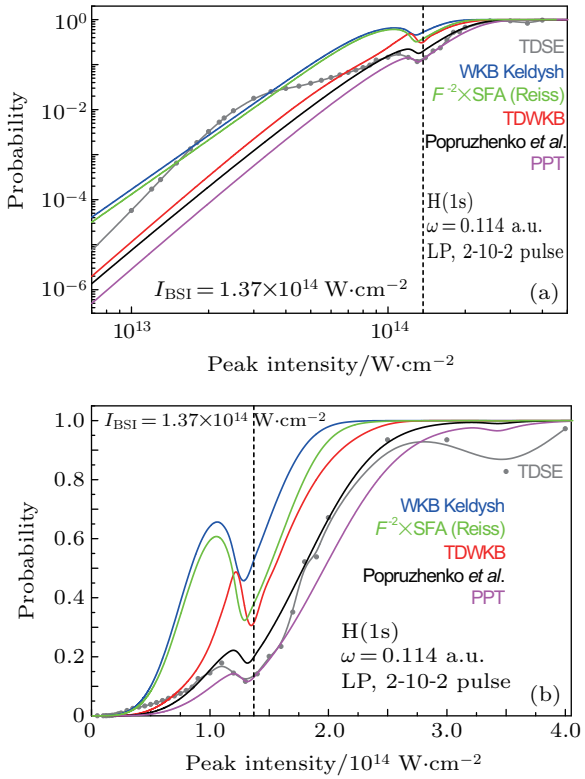


Fig. 6. (color online) The same caption as that in Fig. 5 but for $\omega = 0.114$ a.u. TDSE data are the same as those in Fig. 2, where (a) both axes are logarithmical and (b) both axes are linear.

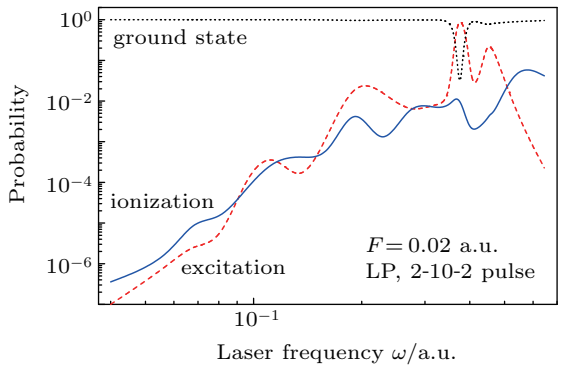


Fig. 7. (color online) Curves of probability of ground state (black dotted curve), ionization (blue solid curve) and excitation (red dashed curve) of H(1s) atom after the end of the laser pulse versus laser frequency ω for $F = 0.02$ a.u. There are exact numerical TDSE results presented here (with the help of B-splines).

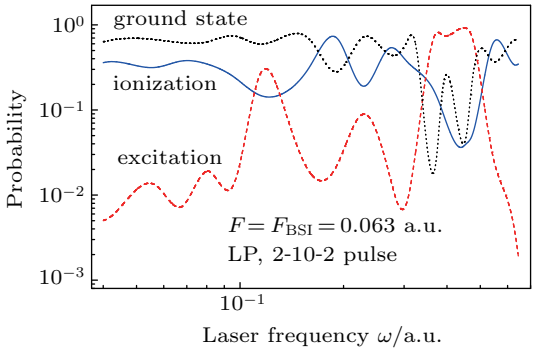


Fig. 8. (color online) The same caption as that in Fig. 7, but for $F = 0.063$ a.u.

frequencies. The first one is near $\omega = 0.114$ a.u., where the states (n,l) with $l = 3$, $l = 1$, and $n = 6,7,8$ dominate after the end of the pulse. The second hump is near $\omega = 0.228$ a.u., where the state $(3,2)$ dominates. A local hump in excitation is usually associated with a local dip in ionization, but the excitation and ionization have comparable probabilities. The ionization probability would be difficult to describe exactly by a single ionization rate formula without taking the excitation into account. One might expect that for frequencies close to the above mentioned values, neglecting the excitation of the atom would overestimate ionization probabilities.

4. Remarks on analytical methods vs. TDSE

In the present work we have compared total ionization probabilities (after the end of the laser pulse) obtained from exact numerical solutions to the TDSE with analogous theoretical predictions based on approximate analytical theories. Such theories give total ionization rates. Under some conditions, by the numerical integration of ionization rates over time, theoretical ionization probabilities can be obtained. There are two possible causes of discrepancies between probabilities computed in these two ways. First of all, using theoretical ionization rates, we have to assume that the excitation is negligible (this does not always hold true, cf. Figs. 7 and 8). Taking into account the presumed theoretical excitation rates would make our description of the process much more complicated. Secondly, the theories that we consider are strong-field or tunneling theories. They have a lower limit of applicability for the field F. For typical visible or near-infrared radiation in the limit $F \to 0$ one goes into (nonresonant) multiphoton ionization regime, where the mechanism of ionization is different.[43] Our work is devoted to the range of laser field parameters where the tunneling mechanism dominates or is at least comparable to the mechanism of multiphoton ionization. Thus, the Keldysh parameter γ changes from values much lower than unity to values of the order of unity. In Figs. 3 and 4 $\gamma \gg 1$ for $F = 0.01$ a.u. (on the left-hand side of the plots). However, for our 2-10-2 pulse, the H(1s) atom starts to ionize in a visible way (1% or so) for $I \geq\sim 5\times10^{13}$ W/cm^2 ($F \geq\sim$ 0.038 a.u.) for $\omega = 0.057$ a.u. and $I \geq\sim 2.5\times10^{13}$ W/cm^2 ($F \geq\sim 0.027$ a.u.) for $\omega = 0.114$ a.u. When it happens $\gamma \approx 1.5$ and $\gamma \approx 4.3$, respectively (probably this is why the agreement between theory and numerical experiment is better in Fig. 5(a) than in Fig. 6(a)). Thus, the tunneling mechanism dominates indeed for most of laser intensities that we consider in Figs. 1 and 2 (particularly for $\omega = 0.057$ a.u.). According to Ref. [44], the dynamic resonances due to Stark level shift in laser fields begin to play a role above $\omega = 2$ eV $= 0.074$ a.u. This is not taken into account in theoretical models which we compare with TDSE results.

The S-matrix theories describing photoionization in intense laser fields usually can be divided into VG and LG theories. They are only approximate and give ionization rates which may differ depending on the gauge. For the TDSE the situation is the opposite. The ionization probabilities which are computed after the end of the pulse, are gauge invariant. In the simplest case, when Coulomb effect is neglected in the final state of the outgoing electron, the ionization probability amplitudes in the above-mentioned two gauges are (cf. Eqs. (8), (9), and appendix B in Ref. [45] and Ref. [36]) as follows:

$$(S-1)_{\rm fi}^{\rm LG} = {\rm i}\int_{-\infty}^{\infty} {\rm d}t\tilde{\Phi}_{\rm i}\left(\boldsymbol{p}+\frac{1}{c}\boldsymbol{A}(t)\right) \times\left(\frac{1}{2}\left(\boldsymbol{p}+\frac{1}{c}\boldsymbol{A}(t)\right)^2+E_{\rm B}\right) \times\exp\left[\frac{\rm i}{2}\int_{-\infty}^{t}\left(\boldsymbol{p}+\frac{1}{c}\boldsymbol{A}(\tau)\right)^2{\rm d}\tau+{\rm i}E_{\rm B}t\right], \quad (9)$$

$$(S-1)_{\rm fi}^{\rm VG} = {\rm i}\int_{-\infty}^{\infty} {\rm d}t\tilde{\Phi}_{\rm i}(\boldsymbol{p})\left(\frac{p^2}{2}+E_{\rm B}\right) \times\exp\left[\frac{\rm i}{2}\int_{-\infty}^{t}\left(\boldsymbol{p}+\frac{1}{c}\boldsymbol{A}(\tau)\right)^2{\rm d}\tau+{\rm i}E_{\rm B}t\right], \quad (10)$$

where $\tilde{\Phi}_{\rm i}(\boldsymbol{p})$ is the initial-state wave function in the momentum representation. Note that the probability amplitude $(S-1)_{\rm fi}^{\rm LG}$ is only a function of the kinetic momentum $\boldsymbol{\pi}(t) = \boldsymbol{p}+\boldsymbol{A}(t)/c$ of the outgoing electron. The probability amplitude $(S-1)_{\rm fi}^{\rm VG}$ depends on the kinetic momentum $\boldsymbol{\pi}(t)$ in the exponential factor and on the canonical momentum $\boldsymbol{p}$ in the pre-exponential factor. (Equation (9) refers to the Keldysh-type theory[1,2] and equation (10) refers to the Reiss theory.[10]) Therefore, a form of the VG amplitude is somehow inconsistent. The VG amplitude is also a result of some hybrid procedure from the gauge standpoint.[46,47] There are at least two meaningful consequences of the qualitative difference between calculations based on ionization amplitudes in the LG and in the VG. First, in Ref. [48] it was shown that one obtains qualitatively conflicting answers in both gauges for the

ionization of negative ions with a ground state of odd parity. And this is the LG that matches the exact (gauge-invariant) numerical solution to the TDSE in this case. It was explained that making the same approximation in two gauges may correspond to different approximations physically and they opt for $\boldsymbol{\pi}(t)$ rather than $\boldsymbol{p}$ in the pre-exponential factor of the ionization amplitude.[48] Secondly, when $F = \text{const}$ (F denotes the field amplitude for any polarization) and $\omega \to 0$ for the hydrogen atom in the initial state with $n = 1$ or $n = 2$ (n is the principal quantum number) one obtains ionization rate which goes to zero if Eq. (10) is used.[49–51] This is true both for the linear[49] and circular polarization[50] of incident radiation. However, the limit $\omega \to 0$ (when the field amplitude $F = \text{const}$ and $\gamma \to 0$) does not mean that there is no electric field. This limit in the theory which is nonrelativistic and uses the dipole approximation, corresponds to quasistatic electric field (the magnetic field is zero). Obviously, any atom does break up with nonzero ionization rate in such a field. Thus, the prediction of the VG S-matrix theory is unphysical in this case. In practice, the lower the value of ω, the higher the discrepancy between the VG ionization rate and the real ionization rate will be. A striking example of such a discrepancy is presented in Fig. 5 of Ref. [36]. The above-mentioned facts (see also Section VI in Ref. [36] for a broader discussion) leads us to prefer LG S-matrix theories.

Different predictions of both gauges in S-matrix theory may be less pronounced if Coulomb effect in the final state of the outgoing electron is taken into account. Note that in Figs. 3, 4, 5(a), and 6(a), the curves showing WKB Keldysh (blue ones) and $F^{-2}\times$ SFA (Reiss; green ones) are very close to each other. These two models utilize the same simple Coulomb correction (in the Gordon–Volkov wave function) in the LG and in the VG, respectively (although the latter model uses some further simplification[38]).

With the help of imaginary time method, Coulomb effect for the ionization in quasistatic laser field has been taken into account in PPT theory.[3–8] The latter uses the quasiclassical wave function for describing the electron in the tunneling domain and matches this wave function to the exact bound-state wave function. The PPT theory (a gauge-invariant approach) is both deeper and more general than the KFR theory, but the former is technically more complicated.[52] According to the authors of Ref. [44] for $\omega = 1.55$ eV$= 0.057$ a.u. the PPT well describes (both qualitatively and quantitatively) total ionization rate of the H(1s) atom up to $\gamma \approx 1.5-2$, which is equivalent to $F \gtrsim 0.03$ a.u. and $I \gtrsim 3\times 10^{13}$ W/cm^2. Our results shown in Fig. 5 confirm this statement. Little better agreement with TDSE in Fig. 5 is found for improved PPT theory.[19] It seems that the advantage of PPT, Popruzhenko *et al.*,[19] and recently introduced TDWKB[35] theories over the remaining two models relies also on the fact that the latter two ones use Coulomb corrections, which are constant in time. Therefore, in the WKB Keldysh and $F^{-2}\times$ SFA (Reiss) models the Coulomb effects are all the time the same as in the moments of peak laser field. The PPT (original or improved) ionization rates are much easier to calculate numerically than the TDWKB ones, which require the computation of generalized Bessel functions for large orders or arguments (particularly if $\omega \ll 0.1$ a.u.).

We have also examined numerical values of ionization rates of the H(1s) atom for two VG S-matrix theories. The first one was published some time ago by one of us (J.H.B.[37] for both circular and linear polarization (cf. Eq. (9b) therein for the respective ionization rate formula). The second one was published recently in this journal[53] (cf. Eq. (21) therein). It appears that for laser field parameters from Figs. 3 and 4 our result is numerically very similar to that from the WKB Keldysh and quite similar to that from the $F^{-2}\times$ SFA (Reiss) theories (see blue and green curves in these figures). The remarkably simple formula from Ref. [53] is numerically usually quite close to the PPT theory. However, it appears that Eq. (21) from Ref. [53] cannot be used when $B \geq 1$ (cf. Eqs. (16) and (21) therein) and the applicability range of this model is smaller than the models from Ref. [37] . For the H(1s) atom the condition $B < 1$ is equivalent to $1.5F\left(1+\gamma^2\right)^2 < 1$. When $\gamma \ll 1$ one obtains $F <\sim 2/3$ from the latter inequality, which does not give a new limitation for F since already one knows that $F \leq\sim F_{\text{BSI}}$. But, for larger value of Keldysh parameter γ, a lower limit appears for the peak field F. For example, for $\omega = 0.057$ a.u. one obtains $F >\sim 0.03$ a.u. and for $\omega = 0.114$ a.u. one obtains $F >\sim 0.085$ a.u. from the condition $B < 1$.

5. Conclusions

Note that for infrared linearly polarized laser radiation of wavelengths longer than about 1064 nm, ionization probability of the H(1s) atom may be quite well described by integrating static electric field ionization rates over the laser pulse profile through using simple empirical formula of Tong and Lin (cf. Fig. 5 in Ref. [27]). This can be called the adiabatic approximation. In the range of shorter laser wavelengths: 250 nm$\leq \lambda \leq$ 1000 nm the adiabatic approximation is valid, but only for peak laser fields $F \gtrsim 0.1$ a.u.,[54] where exact numerical static electric field ionization rates have been used.[55,56]

In this work we have investigated ionization (mainly) and excitation (only to some extent) of the H(1s) atom in typical visible or near-infrared radiation. The range of laser field intensities that we have taken into account is related to the probability of ionization for cw laser pulse (with 10-cycles flat part). In our case the ionization probability changes from at least

10^{-5} (or less) to 1. Thus, the laser field changes from perturbative to nonperturbative field. If one considers only ionization probability, nonrelativistic dipole approximation is sufficient. Before reaching the intensity of about 4.0×10^{14} W/cm^2, the H(1s) atom becomes fully ionized for the above-mentioned laser pulse and wavelengths. The results from the well-known theoretical models describing the ionization rate are in satisfactory qualitative and sometimes also quantitative agreement with the exact numerical results. Better agreement with TDSE is achieved for lower frequencies (greater wavelengths). For higher frequencies, particularly for such a frequency that the resonant excitation is probable, the excitation may be stronger (even much stronger) than the ionization. For lower intensities (and ionization probabilities much lower than 1) the best theoretical models, providing simple ionization rate formula, are WKB Keldysh and $F^{-2}\times$ SFA (Reiss) theories. For higher peak intensities, near $I_{\rm BSI} = 1.37 \times 10^{14}$ W/cm^2 and above, the model of Popruzhenko *et al.* and the model of PPT better describe ionization probabilities when the real ionization probability is significant ($\geq\sim 0.1$). Application of TDWKB theory typically leads to the underestimation of ionization probabilities when they are small, and the overestimation of them when they are significant. The TDWKB ionization rates usually lie between the smallest and the highest theoretical ionization rates, but they are closest to the model of Popruzhenko *et al.*

Acknowledgment

We would like to thank Prof. Hong Ping Liu and Prof. Dieter Bauer for helpful discussion on our computer program.

References

[1] Keldysh L V 1964 *Zh. Eksp. Teor. Fiz.* **47** 1945
[2] Keldysh L V 1965 *Sov. Phys.- JETP* **20** 1307
[3] Perelomov A M, Popov V S and Terent'ev M V 1966 *Zh. Eksp. Teor. Fiz.* **50** 1393
[4] Perelomov A M, Popov V S and Terent'ev M V 1966 *Sov. Phys.- JETP* **23** 924
[5] Perelomov A M, Popov V S and Terent'ev M V 1966 *Zh. Eksp. Teor. Fiz.* **51** 309
[6] Perelomov A M, Popov V S and Terent'ev M V 1967 *Sov. Phys.- JETP* **24** 207
[7] Perelomov A M and Popov V S 1967 *Zh. Eksp. Teor. Fiz.* **52** 514
[8] Perelomov A M and Popov V S 1967 *Sov. Phys.- JETP* **25** 336
[9] Faisal F H M 1973 *J. Phys. B: At. Mol. Phys.* **6** L89
[10] Reiss H R 1980 *Phys. Rev. A* **22** 1786
[11] Reiss H R 1992 *Prog. Quantum Electron.* **16** 1
[12] Gribakin G F and Yu M 1997 *Phys. Rev. A* **55** 3760
[13] Popov V S 2004 *Usp. Fiz. Nauk* **174** 921
[14] Popov V S 2004 *Phys. Usp.* **47** 855
[15] Becker A and Faisal F H M 2005 *J. Phys. B: At. Mol. Opt. Phys.* **38** R1
[16] Milošević D B, Paulus G G, Bauer D and Becker W 2006 *J. Phys. B: At. Mol. Opt. Phys.* **39** R203
[17] Popruzhenko S V 2014 *J. Phys. B: At. Mol. Opt. Phys.* **47** 204001
[18] Bauer D and Mulser P 1999 *Phys. Rev. A* **59** 569
[19] Popruzhenko S V, Mur V D, Popov V S and Bauer D 2008 *Phys. Rev. Lett.* **101** 193003
[20] Ammosov M V, Delone N B and Krainov V P 1986 *Zh. Eksp. Teor. Fiz.* **91** 2008
[21] Ammosov M V, Delone N B and Krainov V P 1986 *Sov. Phys. JETP* **64** 1191
[22] Fu Y Z, Zhao S F and Zhou X X 2012 *Chin. Phys. B* **21** 113101
[23] Zhao S F, Le A T, Jin C, Wang X and Lin C D 2016 *Phys. Rev. A* **93** 023413
[24] Dörr M, Potvliege R M and Shakeshaft R 1990 *Phys. Rev. Lett.* **64** 2003
[25] Shakeshaft R, Potvliege R M, Dörr M and Cooke W E 1990 *Phys. Rev. A* **42** 1656
[26] Krainov V P, Xiong W and Chin S L 1992 *Laser Phys.* **2** 467
[27] Tong X M and Lin C D 2005 *J. Phys. B: At. Mol. Opt. Phys.* **38** 2593
[28] Krainov V P and Shokri B 1995 *Zh. Eksp. Teor. Fiz.* **107** 1180
[29] Krainov V P and Shokri B 1995 *Sov. Phys.- JETP* **80** 657
[30] Krainov V P 1997 *J. Opt. Soc. Am. B* **14** 425
[31] Tong X M and Chu S I 1997 *Chem. Phys.* **217** 119
[32] Bauer D and Koval P 2006 *Comput. Phys. Commun.* **174** 396
[33] Gordon W 1926 *Z. Phys.* **40** 117
[34] Volkov D M 1935 *Z. Phys.* **94** 250
[35] Bauer J H 2017 *J. Phys. B: At. Mol. Opt. Phys.* **50** 085601
[36] Bauer J 2006 *Phys. Rev. A* **73** 023421
[37] Bauer J H 2007 *Phys. Rev. A* **75** 045401
[38] Becker A, Plaja L, Moreno P, Nurhuda M and Faisal F H M 2001 *Phys. Rev. A* **64** 023408
[39] Reiss H R 2002 *Phys. Rev. A* **65** 055405
[40] Brunetti E, Becker W, Bryant H C, Jaroszynski D A and Chou W 2015 *New J. Phys.* **17** 053008
[41] Bauer J H 2010 *Phys. Rev. A* **81** 013414
[42] Bauer J H 2016 *J. Phys. B: At. Mol. Opt. Phys.* **49** 145601
[43] Klaiber M and Briggs J S 2016 *Phys. Rev. A* **94** 053405
[44] Volkova E A, Gridchin V V, Popov A M and Tikhonova O V 2006 *JETP* **102** 40
[45] Bauer J H 2008 *J. Phys. B: At. Mol. Opt. Phys.* **41** 185003
[46] Burlon R, Leone C, Trombetta F and Ferrante G 1987 *Nuovo Cimento D* **9** 1033
[47] Leone C, Bivona S, Burlon R, Morales F and Ferrante G 1989 *Phys. Rev. A* **40** 1828
[48] Bauer D, Milošević D B and Becker W 2005 *Phys. Rev. A* **72** 023415
[49] Vanne Yu V and Saenz A 2007 *Phys. Rev. A* **75** 033403
[50] Bauer J H 2011 *Phys. Rev. A* **83** 035402
[51] Bauer J H 2011 *Phys. Rev. A* **84** 025403
[52] Ivanov M and Smirnova O 2012 *Ionization Strong Low-Frequency Fields: From Quantum S-Matrix Class. Pictures*, June 11–15, 2012, Corinf School, Dresden, Germany
[53] Li J, Huo Y N, Tang Z H and Ma F C 2017 *Chin. Phys. B* **26** 023203
[54] Scrinzi A, Geissler M and Brabec T 1999 *Phys. Rev. Lett.* **83** 706
[55] Scrinzi A 2000 *Phys. Rev. A* **61** 041402(R)
[56] Scrinzi A, private communication